Electronic Supplementary Material (ESI) for Journal of Materials Chemistry A.


# ·Supporting Information

# Ultrahigh Effective $H_2/D_2$ Separation in an Ultramicroporous Metal-organic Framework Material through Quantum Sieving

Dawei Cao,[a,b,†] Hongliang Huang,[c,†] Youshi Lan,[d] Xiaojun Chen,[a] Qingyuan Yang,[d] Dahuan Liu,[d] Yu Gong,[a] Chengjian Xiao,[a] Chongli Zhong*[c,] and Shuming Peng*[a]

[a.] *Institute of Nuclear Physics and Chemistry, China Academy of Engineering Physics, Mianyang, Sichuan, 621900, China. Email: pengshuming@caep.cn*

[b.] *Department of Engineering Physics, Tsinghua University, Beijing 100084, China.*

[c.] *State Key Laboratory of Separation Membranes and Membrane Processes, Tianjin Polytechnic University, Tianjin 300387, China. Email: zhongchongli@tipu.edu.cn*

[d.] *State Key Laboratory of Organic-Inorganic Composites, Beijing University of Chemical Technology, Beijing 100029, China*

[†] *These authors contributed equally to this work.*

TABLE OF CONTENTS

given exposure temperature and loading pressure.

*Experimental Section*

**Preparation and characterization of AHEFAU:**

The AHEFAU MOF was synthesized according to previous report[1]. Typically, 3.00 g of $FeCl_3 \cdot 6H_2O$, 1.2 g of NaOH, 1.80 g of benzenetetracarboxylic acid, and 0.3 g of MgO were mixed in 20 ml $H_2O$ in a 30 ml Teflon lined reactor. After sonication for 10 min, the Teflon lined vessel was sealed and placed in a preheated oven at 160 °C for 72 h. After cooling to room temperature, the resultant brown crystals were filtrated and washed with distilled water.

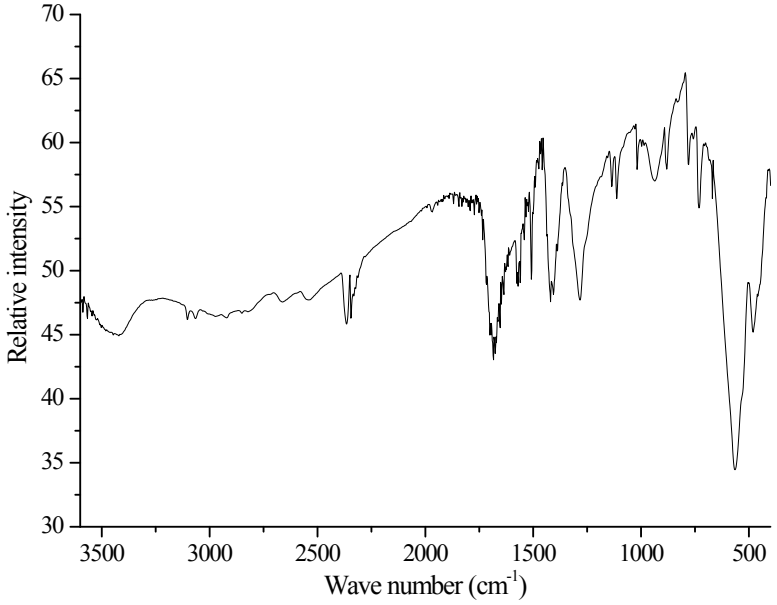


**Figure S1.** IR spectrum of AHEFAU. The peaks around 1700 $cm^{-1}$ correspond to the typical Ar-COO- frequencies.

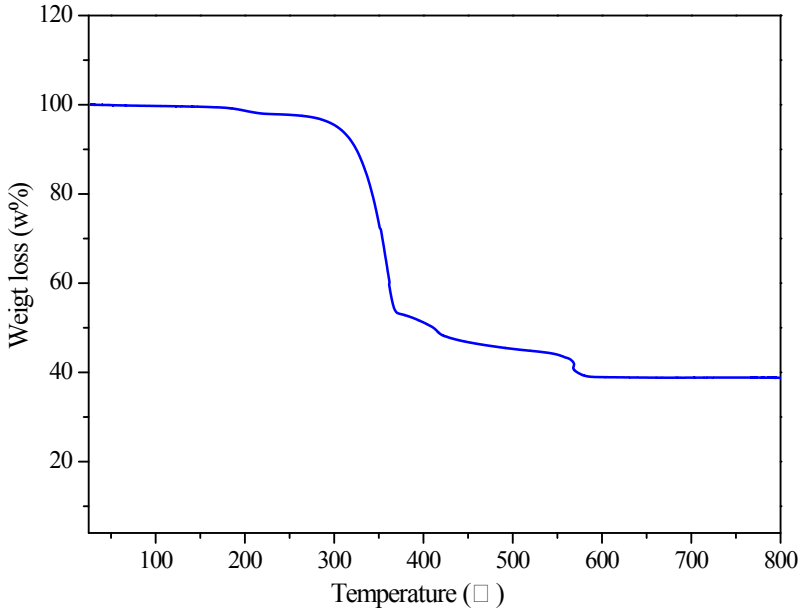


**Figure S2.** TGA profile of AHEFAU. The weight loss occurring between 30 and 250 °C corresponds to the loss of small water molecules, the framework collapses above 300 °C.

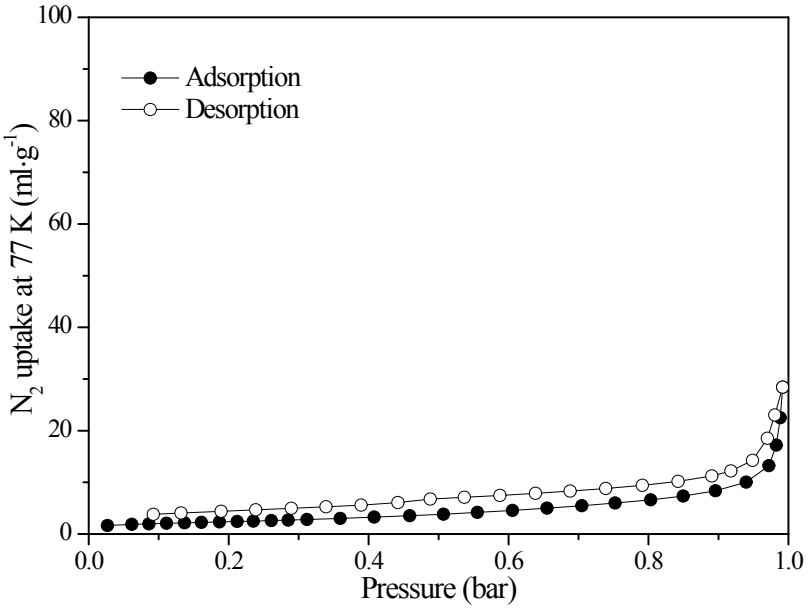


**Figure S3.** $N_2$ adsorption-desorption isotherm at 77 K of AHEFAU which shows a complete exclusion of $N_2$, the rise at higher pressure is ascribed to the occurrence of multilayer adsorption at the exterior surface and the powder interstices.

**Advanced cryogenic thermal desorption spectroscopy (ACTDS) apparatus and TDS measurement procedure for the quantum sieving of $H_2/D_2$ mixture**

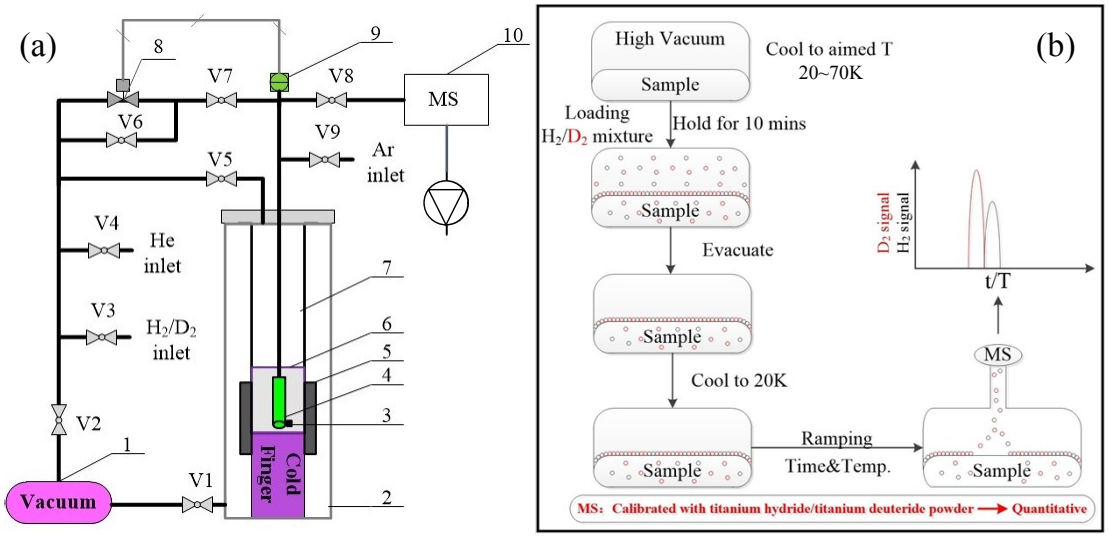


**Figure S4.** a) Advanced cryogenic thermal desorption spectroscopy (ACTDS) apparatus. The indexed parts are: vacuum system (1), vacuum isolator (2), thermocouple (3) attached to the bottom of the sample chamber (4), heater (5), cold trap made of copper (6), cold trap made of stainless steel (7), electromagnetic valve (8) coupled with pressure transducers (9), quadrupole MS with turbo molecular pump (10), and ball valves (V1, V2, V3, V4, V5, V6, V7, V8, V9). b) TDS measurement procedure for the quantum sieving of $H_2/D_2$ mixture.

**ACTDS apparatus:**

An ACTDS apparatus was designed after that of the Max Planck Institute[2, 3] for the ultralow-temperature QS investigations of hydrogen isotopes (figure S4a). The sample chamber (4), made of

stainless steel, with a thermocouple (3) attached to its lower-most part in order to warrant a precise temperature measurement of the sample, is suspended in a cold trap made of copper (6) connected directly to a cold trap made of stainless steel (7) which is designed to maintain a homogeneous temperature in the copper made one, both cold traps are filled with a certain pressure of pure helium; the copper made cold trap (6) is connected directly to the cold finger of a liquid helium flow cryostat which allows to cool to a temperature of less than 4 K; surrounding the copper made cold trap (6) and the upper-most part of the cold finger is a circle of an ancillary resistive heater block (5) that can achieve a temperature of 425 K with adjustable heating rate; outside the whole part there is a vacuum chamber (2) for isolation; the vacuum of the apparatus is provided by a turbine molecular pump (1) which can achieve an ultimate vacuum of $10^{-6}$~$10^{-7}$ Pa; the $H_2/D_2$ mixture is dosed into the sample chamber automatically through a computer-controlled electromagnetic valve (8) coupled with two pressure transducers (9) with ranges of $10^{-4}$~1 Torr (CDG025D, Inficon) and 0.1~$10^3$ Torr (CDG025D, Inficon) and an accuracy of 0.2% of indication; the adsorbed gases are analyzed by a quadrupole MS (10), which detects masses in the range from 1 to 100 amu with time and possesses a sensitivity of $2\times10^{-14}$ Torr.[4]

**Experiment procedure for $H_2/D_2$ quantum sieving—TDS:**

We carried out our $H_2/D_2$ quantum sieving experiment following a procedure recommended by the Max Planck Institute (figure 4b):[2, 5-8] First, 39 mg of AHEFAU having been activated for 12 h at 100 ℃ under high vacuum (final pressure <$10^{-4}$ Pa) in the sample chamber was cooled down to the experimental temperature (20 K, 30 K, 40 K, 50 K, 60 K and 70 K) under high vacuum. Then, a defined pressure (0.2 kPa, 0.5 kPa, 1.0 kPa, 3.0 kPa and 5.0 kPa) of the $H_2/D_2$ mixture (feeding gas $H_2$: $D_2$=1: 0.8594) was dosed into the sample chamber. After 10 min's competitive saturated adsorption (figure S8), the gas molecules that had not been adsorbed were pumped out. Afterwards, the sample was cooled down to a temperature lower than 20 K. Finally, the thermally activated desorption procedure was applied with a simultaneous recording of the desorbed $H_2/D_2$ signal by the quadrupole MS, which, after careful calibration, can give out a quantified amount of the desorbed $H_2/D_2$ gases (right proportional to the area under the desorption curve).[4] While, as the sample chamber is suspended in a pure helium environment in the copper made cold trap, heat transfer from both the cold finger and the ancillary resistive heater block is indirect to the sample chamber; therefore, though a linear ramping rate was set, the real heating ramp of the thermally activated desorption procedure is somewhat shift from linear. For the TDS procedures at $T_{exp}$=40 K, 50 K, 60 K and 70 K, a ramping program shown in figure S5 was applied; while, due to an enhancement in adsorption capacity at $T_{exp}$=20 K, the ramping program shown in figure S5 resulted in a signal overrun of the quadrupole MS, hence, a ramping program of a smaller heating rate shown in figure S6 was applied for all exposed pressures at $T_{exp}$=20 K; for the experiments at $T_{exp}$=30 K, the cold traps filled with pure helium was accidently doped with/leaked into a small amount of air, leading to a disturbance in the ramping program at the TDS temperature of 56 K (figure S7), thus, reflecting on the TDS spectra (figure S9), one can obviously observe that differences in shapes between TDS spectra at $T_{exp}$=30 K and that at $T_{exp}$=40 K, 50 K, 60 K and 70 K exist (figure S9). To eliminate these differences, the cold traps were substituted with fresh pure helium and experiments at $T_{exp}$=30 K were repeated, with the same ramping program as shown in figure S5. After substitution, TDS spectra at $T_{exp}$=30 K (0.2 kPa, 0.5 kPa, 1.0 kPa) showed a consistence in shape with those at $T_{exp}$=40 K, 50 K, 60 K and 70 K, however, with an enhancement in the adsorption capacity under higher pressures (≥3 kPa) at $T_{exp}$=30 K, the ramping program shown in figure S5

resulted in a signal overrun of the quadrupole MS, the same situation as met in the experiments at $T_{exp}$=20 K, thus, to maintain a consistency of the TDS ramping program, we retained the TDS spectra at $T_{exp}$=30 K with the ramping program shown in figure S7.

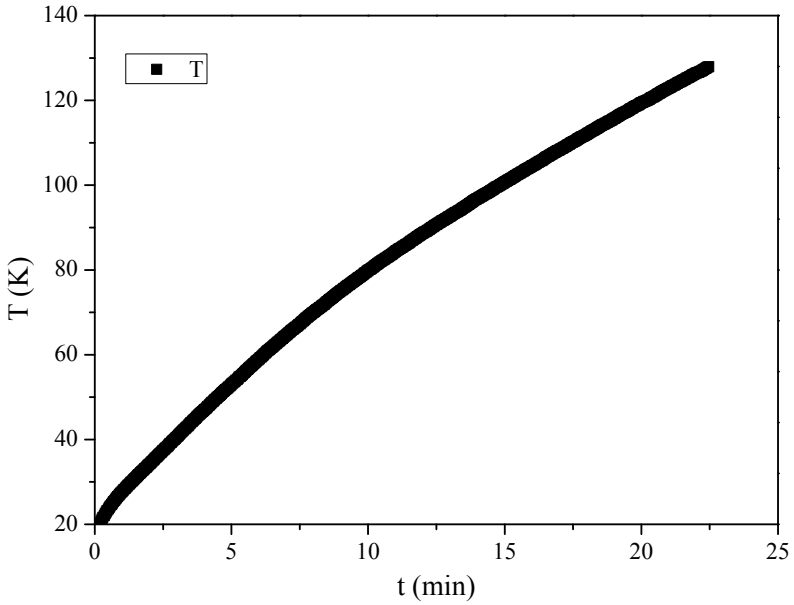


**Figure S5.** Ramping program for the $H_2/D_2$ TDS experiments at $T_{exp}$=40 K, 50 K, 60 K and 70 K.

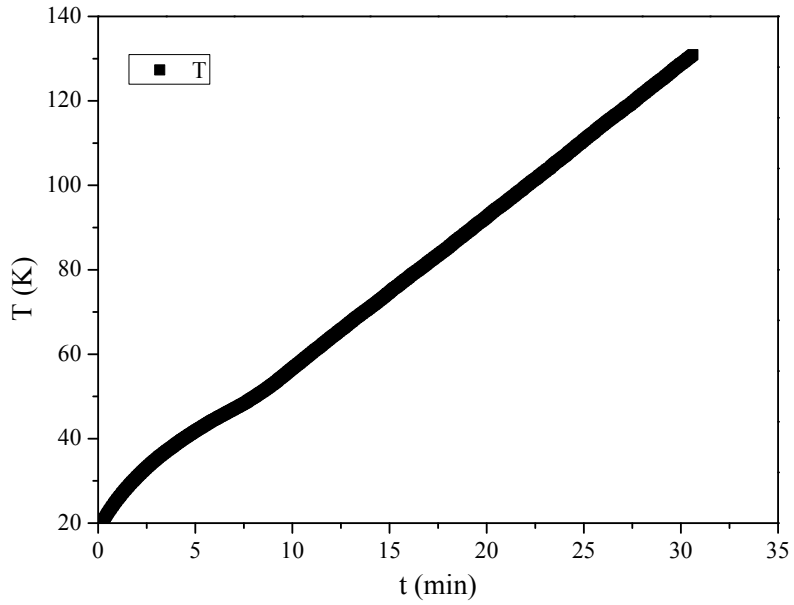


**Figure S6.** Ramping program for the $H_2/D_2$ TDS experiments at $T_{exp}$=20 K.

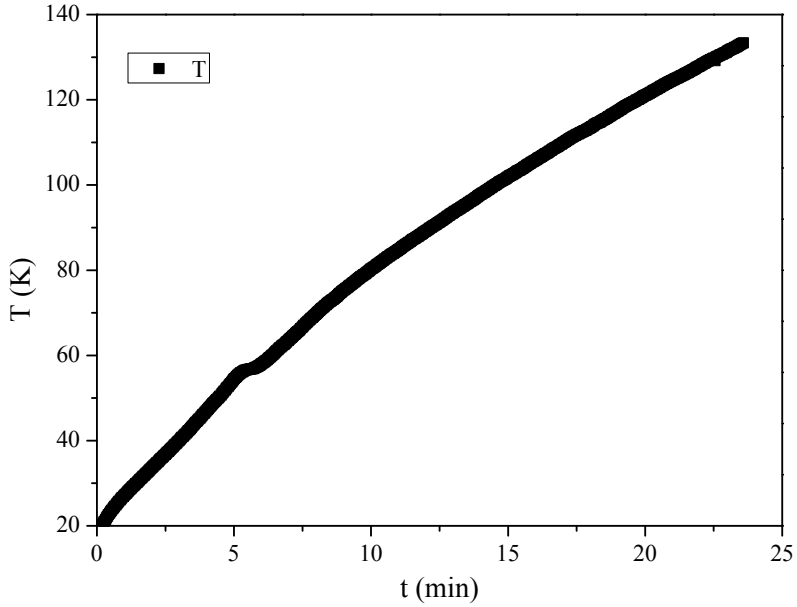


**Figure S7.** Ramping program for the $H_2/D_2$ TDS experiments at $T_{exp}$=30 K.

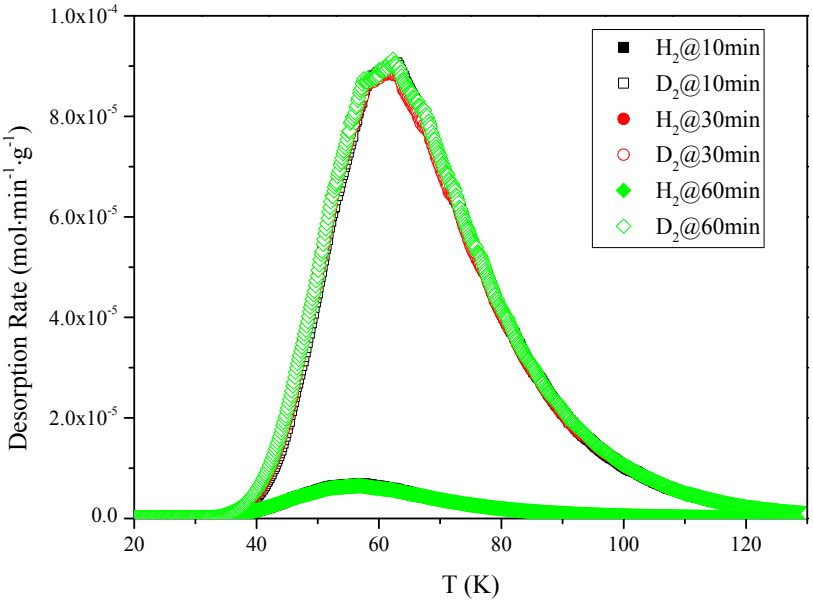


**Figure S8.** Time dependence of the TDS spectra @$T_{exp}$=40 K and a pressure of 3.0 kPa during gas mixture exposure. TDS spectra under different exposure time: 10 mins (square, solid (■) for $H_2$ and open (□) for $D_2$), 30 mins (circle, solid (●) for $H_2$ and open (○) for $D_2$) and 60 mins (diamond, solid (◆) for $H_2$ and open (◇) for $D_2$) coincide almost identical with each other, which shows that an experimental exposure time of 10 mins is sufficient for a competitive saturated adsorption that results in an EQS result.

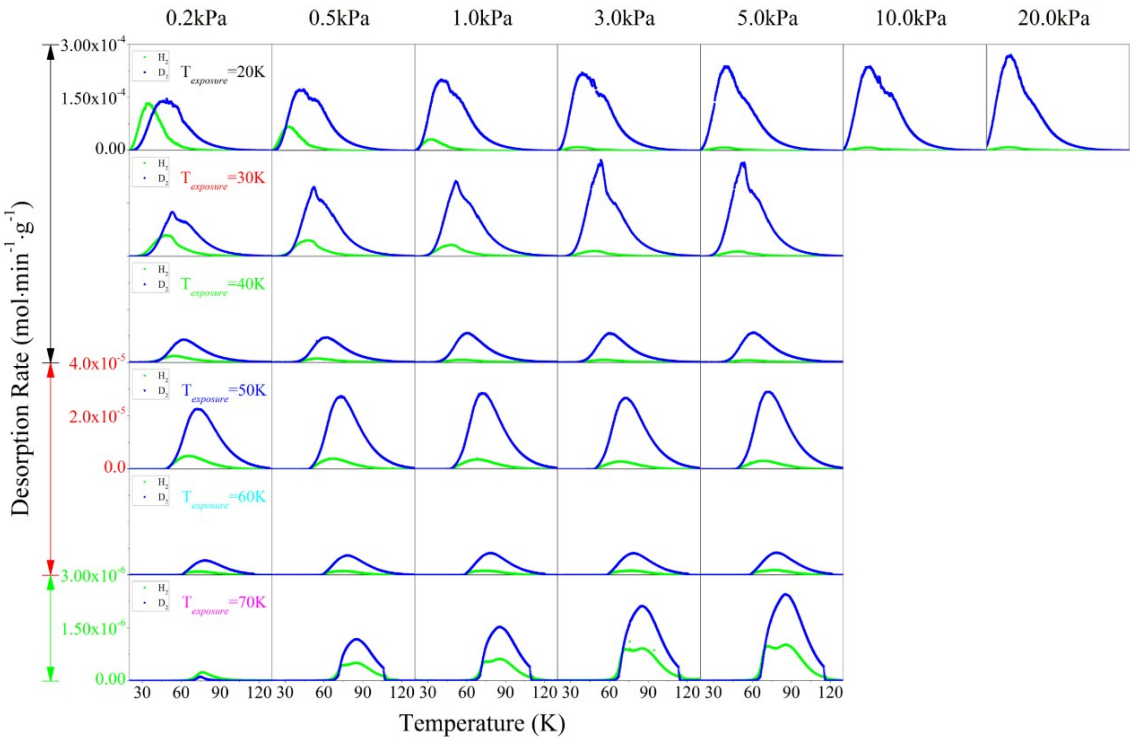


**Figure S9.** $H_2$ (green)/$D_2$ (blue) TDS spectra (with non-rigorous linear ramping rates) of AHEFAU at loading pressures of 0.2 kPa, 0.5 kPa, 1.0 kPa, 3.0 kPa, 5.0 kPa, 10.0 kPa (for $T_{exp}$=20 K only) and 20.0 kPa (for $T_{exp}$=20 K only) (feeding gas $H_2$: $D_2$=1: 0.8594) under different exposure temperatures: 20 K (■), 30 K (●), 40 K (▲), 50 K (▼), 60 K (◆) and 70 K (★).

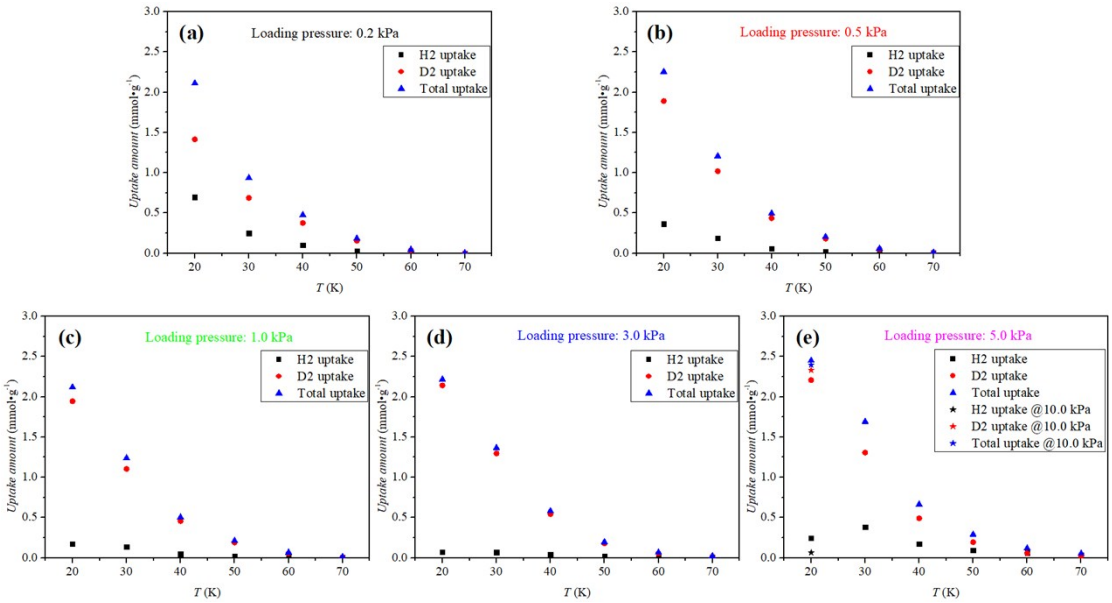


**Figure S10.** $H_2$, $D_2$ and total ($H_2$+$D_2$) gas uptake of $H_2$/$D_2$ mixture (feeding gas $H_2$: $D_2$=1: 0.8594) as a function of $T_{exp}$ for different loading pressures: (a) 0.2 kPa, (b) 0.5 kPa, (c) 1.0 kPa, (d) 3.0 kPa and (e) 5.0 kPa with 10.0 kPa at 20 K also shown.

**Table S1**. Separation performance ($SF_{D_2/H_2}$) of the $D_2/H_2$ mixture (feeding gas $H_2$: $D_2$=1: 0.8594) at given exposure temperature and loading pressure.

| Pressure (kPa) | Separation factor ($(n_{D_2}/n_{H_2})/(y_{D_2}/y_{H_2})$) | | | | | |
|---|---|---|---|---|---|---|
| | **20 K** | **30 K** | **40 K** | **50 K** | **60 K** | **70 K** |
| **0.2** | 2.5 ± 0.2 | 3.2 ± 0.1 | 4.7 ± 0.4 | 6.2 ± 0.0 | 4.9 ± 0.0 | 0.2 ± 0.1 |
| **0.5** | 6.4 ± 0.4 | 6.6 ± 0.3 | 9.0 ± 0.3 | 9.1 ± 0.0 | 5.9 ± 0.0 | 2.4 ± 0.0 |
| **1.0** | 13.6 ± 0.7 | 10.1 ± 0.7 | 11.2 ± 0.1 | 9.9 ± 0.0 | 5.6 ± 0.0 | 2.6 ± 0.0 |
| **3.0** | 32.3 ± 1.2 | 21.4 ± 0.0 | 15.9 ± 0.5 | 11.5 ± 0.0 | 5.5 ± 0.0 | 2.3 ± 0.0 |
| **5.0** | 38.4 ± 1.6 | 23.6 ± 0.0 | 18.1 ± 0.6 | 11.6 ± 0.0 | 5.0 ± 0.0 | 2.5 ± 0.0 |
| **10.0** | 41.4 ± 0.4 | | | | | |
| **20.0** | 40.6 ± 0.5 | | | | | |

Please note that not all experiments under each pressure at each exposed temperature were repeated, the values in boxes were the ones that were repeated.

**Verification of our ACTDS apparatus: repeated experiments**

To verify the validity of the data we obtained from our ACTDS apparatus, we tried to repeat the reported results for $D_2/H_2$ separation in CPO-27-Co with the same operational conditions as in reference 6. Finally, a selectivity of 12.1±0.1 with a corresponding adsorbed $D_2$ amount of 2.88±0.27mmol/g under 3.0 kPa at 60 K was repeated, which agree almost identically with the values in reference 6, well verifying the validity of our ACTDS apparatus. (Figure S11)

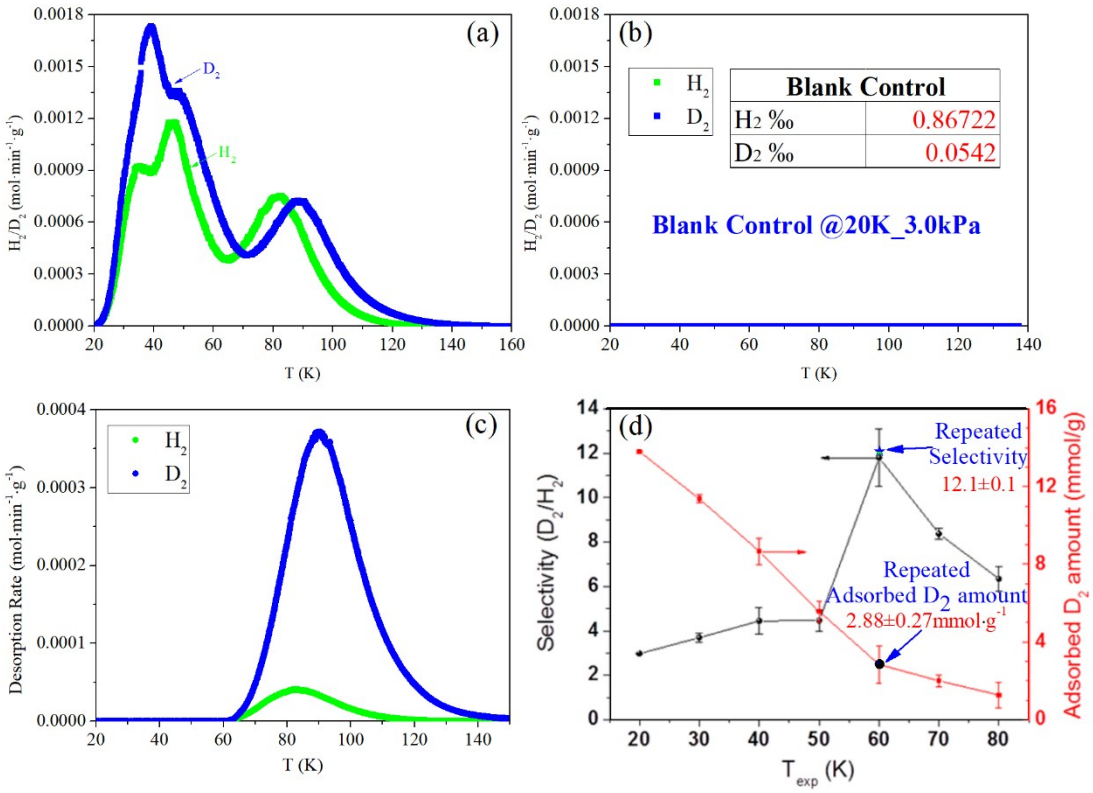


**Figure S11.** a) Repeated pure $H_2$ and $D_2$ thermal desorption spectra of CPO-27-Co at a loading pressure of 3.0 kPa @$T_{exp}$=20 K. b) Blank control of pure $H_2$ and $D_2$ thermal desorption spectra of

CPO-27-Co at a loading pressure of 3.0 kPa @$T_{exp}$=20 K with the relevant deviation also shown. c) Repeated mixed $H_2/D_2$ (feeding gas $H_2$: $D_2$=1: 0.8594) thermal desorption spectra of CPO-27-Co at a loading pressure of 3.0 kPa @$T_{exp}$=60 K. d) Comparison of the repeated selectivity and relevant adsorbed $D_2$ amount of CPO-27-Co at a loading pressure of 3.0 kPa @$T_{exp}$=60 K with those from reference 6, the repeated selectivity and relevant adsorbed $D_2$ amount agreed almost identically with that from reference 6. Note that the ramping rate of our TDS procedure is not rigorously linear, desorption curves of the repeated TDS spectra may show some difference with those from reference 6.

# References:


1. D.-Q. Chu, C.-L. Pan, L.-M. Wang and J.-Q. Xu, *Mendeleev Communications*, 2002, 12, 207-208.
2. H. Oh, S. B. Kalidindi, Y. Um, S. Bureekaew, R. Schmid, R. A. Fischer and M. Hirscher, *Angew Chem Int Ed Engl*, 2013, 52, 13219-13222.
3. H. Oh and M. Hirscher, *European Journal of Inorganic Chemistry*, 2016, 2016, 4278-4289.
4. D. Cao, S. Peng, X. Chen, J. Hou, P. Chen, C. Xiao, Y. Gong and H. Wang, *Analytical Methods*, 2017, 9, 3067-3072.
5. H. Oh, PhD, Max Planck Institute for Intelligent Systems, 2014.
6. H. Oh, I. Savchenko, A. Mavrandonakis, T. Heine and M. Hirscher, *Acs Nano*, 2014, 8, 761-770.
7. J. Y. Kim, R. Balderas-Xicohtencatl, L. Zhang, S. G. Kang, M. Hirscher, H. Oh and H. R. Moon, *J Am Chem Soc*, 2017, 139, 15135-15141.
8. I. Weinrauch, I. Savchenko, D. Denysenko, S. M. Souliou, H. H. Kim, M. Le Tacon, L. L. Daemen, Y. Cheng, A. Mavrandonakis, A. J. Ramirez-Cuesta, D. Volkmer, G. Schutz, M. Hirscher and T. Heine, *Nat Commun*, 2017, 8, 14496.